

## Influence of plasticizers and cryogenic grinding on the high-cooling-rate solidification behavior of PBT/PET blends

Anesh Manjaly Poulouse,<sup>1,2</sup> Stefano Piccarolo,<sup>2</sup> Domenico Carbone,<sup>3</sup> Saeed M. Al-Zahrani<sup>1</sup>

<sup>1</sup>Chemical Engineering Department, P.O. Box 800, King Saud University, Riyadh 11421, Saudi Arabia

<sup>2</sup>INSTM Italy and DICGIM, Università di Palermo, Viale delle Scienze, Palermo, Italy

<sup>3</sup>Istituto di Chimica e Tecnologia dei Polimeri, CNR, Catania

Correspondence to: S. Piccarolo (E-mail: Stefano.piccarolo@unipa.it)

**ABSTRACT:** Two structurally different plasticizers (cyclic and linear) and the effect of cryogenic grinding on the solidification behavior at high cooling rates by a continuous cooling transformation approach of poly(butylene terephthalate)/poly(ethylene terephthalate), PBT/PET, blends are described. The solidification curve (density versus cooling rate) is confirmed as an effective tool to compare the differences in crystallization behavior under conditions mimicking processing. In comparison to the bulky cyclic plasticizer, the linear oligomeric one was found to have a more pronounced influence on the crystallization behavior. A 60/40 by weight PBT/PET blend shows a drop-off of density at  $\sim 50$  K/s. In the plasticized sample, the long-range crystalline order appears up to a cooling rate of  $\sim 250$  K/s, making the blend comparable to pure PBT. Grinding the components before blending further improves crystallizability and synergy to the addition of the plasticizer. The results suggest the important role of local chain mobility in the solidification behavior at high cooling rates. © 2015 Wiley Periodicals, Inc. *J. Appl. Polym. Sci.* **2016**, *133*, 43083.

**KEYWORDS:** blends; crystallization; plasticizer

Received 11 January 2015; accepted 25 October 2015

DOI: 10.1002/app.43083

### INTRODUCTION

In recent years, crystalline/crystalline polymer blends have received significant attention because of their commercial importance and because blending such polymers offers an effective route to widen the range of morphological patterns and to create novel structure–property relationships.<sup>1–3</sup> There are only a few polymer blend systems of two individually crystallizable components with complete miscibility in the melt. One such system is poly(butylene terephthalate)/poly(ethylene terephthalate) (PBT/PET), which is more widely studied because of its commercial importance.<sup>4–11</sup> PET is a comparatively cheap, commercially relevant synthetic engineering thermoplastic, but its crystallization rate is too low to permit reasonable cycle times for injection molding. The PET on blending with PBT will give the processing advantages of PBT, maintain the transparency, retain the basic polyester properties, and find applications in automotive, electrical/electronic, appliances, packaging and in industrial equipment.<sup>12,13</sup>

The miscibility behavior of the blend is crucial for understanding and tailoring the properties relevant for practical application, and the PBT/PET blend system is a good example of intermolecular interactions becoming the key for amorphous phase miscibility.<sup>4,5</sup> Further complications in the solidification

of the PBT/PET blend arise from the possibility that interchange reactions take place between the two constituents, affecting the primary structure of the chain and their crystallizing ability. The miscibility in these polymers, which is improved by the formation of copolymers resulting from intermolecular exchange reactions, has, however, a negative effect on the crystallization. As the interchange reaction proceeds, the blend initially converts to a block copolymer and then finally to a random copolymer that does not crystallize.<sup>14–16</sup> The crystallization process itself is a very sensitive probe of such randomization processes, causing them to be relevant even when NMR methods do not have enough sensitivity for their probing.<sup>17,18</sup>

This work is part of a larger campaign aiming to study the presence of plasticizers and other procedures to improve crystallization behavior and is especially focused on polyesters and their blends at high cooling rates, that is, those mimicking the solidification conditions experienced in processing.<sup>19</sup> The objective of the work is to provide more insights into the complex crystallization process that takes place, especially within the timescale experienced in actual processing.<sup>20</sup> The blend studied uses PBT and PET in a composition equal to a commercial one (60/40 w/w), which has been shown to optimize the crystallization behavior at high cooling rates by using a large proportion of PBT.<sup>11</sup>

**Table I.** Polymer Samples Melt-Mixed for the Study

Samples	Materials
RW00	PBT/PET (60/40 w/w), pellets
GR00	PBT/PET (60/40 w/w), ground
RW5P	PBT/PET (60/40 w/w), pellets + 5 wt % [P] plasticizer
GR5P	PBT/PET (60/40 w/w), ground + 5 wt % [P] plasticizer
GR1P	PBT/PET (60/40 w/w), ground + 1 wt % [P] plasticizer
GR1D	PBT/PET (60/40 w/w), ground + 1 wt % [D] plasticizer
GR5D	PBT/PET (60/40 w/w), ground + 5 wt % [D] plasticizer

It is well known that the PBT/PET system shows amorphous miscibility. Co-crystallization is excluded, at least in the domain of mild cooling conditions, because of the mismatch in their unit cells, and it exhibits the usual melting endotherms of the two components.<sup>5,21–24</sup> In this context and assuming the absence of transesterification reactions, Stocco *et al.* suggested that a preliminary stage of segregation and phase separation (demixing) must occur prior to the onset of separate crystalline units.<sup>11</sup> This mechanism was proposed by comparing the solidification curve of the blend to the ideal behavior model, that is, under the hypothesis of volume additivity, with the result that the overall rate of crystallization of a PBT/PET blend is a measure of the kinetics of this demixing step.<sup>11</sup> A recent work on the influence of plasticizers on PET and PBT suggests the importance of local mobility on polymer solidification, especially at higher cooling rates.<sup>25</sup> It is found that the plasticizer used has a significant effect on the solidification behavior of PET but not on PBT, making PET crystallize faster. The authors suggested that the different behavior of PET and PBT in the presence of a plasticizer must come from them being “stiffer” and “softer” chain polymers, respectively. In this paper the PBT/PET blends, both plasticized and unplasticized, were prepared to understand the role of the particular plasticizer introduced and the mixing conditions. For this purpose, one set was a melt blended with pellets and the other with pulverized components. The solidification curves of the individual components, their blends, and the plasticized ones are compared.

## EXPERIMENTAL

The PET, identified in this work as PET01, is supplied by DSM Engineering Plastics, (Geleen, Netherlands) and has an intrinsic viscosity of 0.62 dl/g in a phenol/tetrachloroethane (60/40) solution at 30°C.

The PBT, identified in this work as PBT02, is also supplied by DSM Engineering Plastics and has an intrinsic viscosity of 0.85 dl/g in a phenol/tetrachloroethane (60/40) solution at 30°C.

The plasticizers used in this work, both soluble with the polymers used, are poly(ethylene glycol) dimethyl ether (PEGDME) [P], an oligomer supplied by Sigma Aldrich (Missouri, United States) (Milan, Italy) with a number-average molecular weight of

$M_n \sim 1,000$ , and dioctyl phthalate (DOP) [D] of molecular weight 390.56 g, having a bulky structure with respect to PEGDME. Both are known to be mutually miscible in the melt state with the polymers studied.<sup>26–28</sup>

Solid CO<sub>2</sub>-assisted grinding of PBT and PET is done before melt blending to a size below 0.1 mm to improve dispersion of the individual moieties. The intrinsic viscosity measurements were carried out to confirm that the pulverization process was not accompanied by any molecular weight change, which could otherwise take place for softer materials.<sup>29</sup> It is worth mentioning that the cryomilled PET has good heat stability in the reheating process, and the serviceability temperature is significantly improved.<sup>30</sup> All of the blends have been melt-mixed in a Brabender Messtechnik GmbH (Duisburg, Germany) mixer (Duisburg, Germany) under a nitrogen blanket at a temperature of 260°C for a mixing time of 4 min and at 50 rpm. The polymers melt-mixed for the study are shown in Table I.

The continuous cooling transformation (CCT) approach and the quenching apparatus setup is described elsewhere.<sup>19</sup> Thin films of 150–200 μm thickness for the quenching experiments were prepared with the help of a hydraulic press by taking an appropriate sample weight and applying a pressure of about 10 MPa. The temperature and holding time were chosen to minimize the trans-esterification reactions. From the thin films, samples of approximately 20×20 mm are cut and wrapped carefully inside aluminum foil. The sample assembly, having a very short thermal response time, is then introduced into the heating zone, heated up to 260°C for 3 min. to remove the thermal history and optimized to minimize transesterification reactions,<sup>11</sup> and then quenched immediately. The effective cooling rate identifying the samples, spanning a range from those obtained by differential scanning calorimetry (DSC) (0.01 to a few K/s) to cooling rates in excess of 1000 K/s, typical of the processing conditions, is measured at 150°C for PBT and PBT/PET blends and at 170°C for PET, corresponding to the temperature at which the maximum kinetic constant is observed when plotted versus temperature.<sup>31</sup> The choice of these temperatures provides a good superposition of the density versus cooling rate data for the DSC and the rapid cooling method of solidification in the domain where both methods can be adopted.<sup>32</sup> Samples are then stored at –10°C to prevent aging. The solidified samples obtained were structurally homogeneous across their thickness and surface width and can be analyzed by macroscopic methods like density, wide-angle X-ray diffraction (WAXD), and so on.<sup>19</sup>

The density measurements are carried out in a gradient column filled with a mixture of carbon tetrachloride and *n*-heptane according to the ASTM D1505 standard test method. The column is calibrated by means of glass beads of known density. The reliability of the results depends on the column preparation, and the gradient should be constant throughout the column. The samples were cut into small pieces, checked for air bubbles by microscope, and degassed under vacuum before being introduced into the gradient column. For each cooling rate, at least three samples are introduced into the column to avoid error propagation. The measurements are taken at 6°C, and the density data are reported at this temperature. The

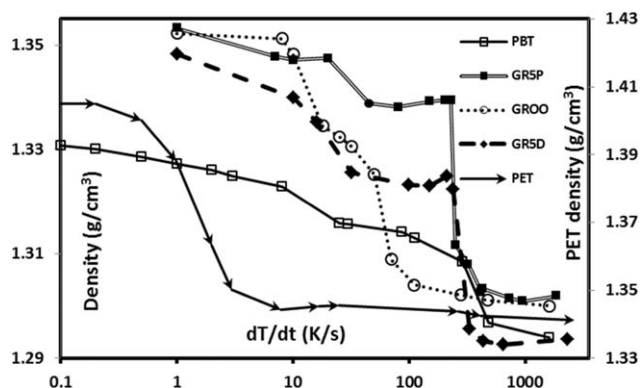


**Figure 1.** Solidification curves of PBT, PET, and the blends GR00 without and GR5P and GR5D with 5% w/w plasticizers. All density values must be read on the left-hand axis except for PET, which is reported on the right-hand axis.

resolution of the density column was 0.0001 kg/L, and repeatability within  $\pm 0.0002$  kg/L was obtained.

The WAXD scans were done in a Bruker Advance D8 X-ray instrument (Massachusetts, USA) (Bruker Italy S.r.l. Milano, Italy) with CuK $\alpha$ -Ni filtered radiation with a wavelength of 0.154 nm within the  $2\theta$  range 12 to 27° with a step of 20 s and a resolution of 0.05° in  $2\theta$ .

DSC data are collected with a power compensation type DSC 7 from Perkin-Elmer (Massachusetts, USA) (Milano, Italy). The instrument is operated in conjunction with liquid nitrogen bath (since the heating was done from  $-40$ ). Approximately 6–8 mg samples are taken in a 20- $\mu$ L aluminum pan and the scanning performed at a rate of 20 K min $^{-1}$  on heating and 10 K min $^{-1}$  on cooling. The heating is carried out from  $-40$  to 280°C.

The dynamic mechanical thermal analysis (DMTA) was performed using a Rheometrics (TA Instruments New Castle, UK) DMTA V (New Jersey, USA) instrument. The heating profile was from  $-20$  to 130°C at a rate of 2 K/min, at a frequency of 10 Hz, under a constant strain amplitude of 0.1%, the minimum for a repeatable result at above the glass-transition temperature ( $T_g$ ), that is, for a sufficient signal-to-noise ratio (S/N) of the stress signal when the modulus drops above the  $T_g$ .

## RESULTS

### Solidification Curves and WAXD Observations: Influence of Plasticizer

The solidification curves of PET, PBT, PBT/PET blend, and the blend with 5 wt % of two different plasticizers are shown in Figure 1, where, being the density span of PET, much larger than the PBT and the blends, the data for PET must be read on the right-hand axis. Although the spread of the data, purposely not smoothed to highlight uncertainties, may complicate the interpretation, the trends of the density dependence with cooling rate of all the compositions studied in this work are clearly outlined. Common features of this data, already described in previous work, can be summarized as follows. There is a constant descent in the density with a slow pace from low cooling rates where crystalline phases are observed; with an increasing cooling rate, the WAXD patterns, shown in Figure 3, broaden,

pointing to a larger disorder and lower crystallite size. A break in the density decrease is observed in a narrow cooling-rate range where stable crystalline phases disappear, and the density suddenly drops. Finally, a lower-density plateau is observed where the WAXD pattern suggests no more crystalline phase to be present except for very small nanocrystals,<sup>33</sup> which significantly affects aging, mechanical properties, and crystallization from the glass.<sup>34</sup>

The PET exhibits a larger density span of 1.405 g/cm $^3$  to 1.335 g/cm $^3$  when plotted as a function of cooling rate than that for PBT, which is from 1.33 g/cm $^3$  to 1.29 g/cm $^3$ .<sup>35</sup> The PBT/PET blend shows a density range of 1.35 g/cm $^3$  to 1.30 g/cm $^3$ , closer to PBT. From Figure 1 it is evident that the PET is a slowly crystallizing material with a density drop at a cooling rate of  $\sim 2$  K/s and PBT at a higher cooling rate of  $\sim 300$  K/s. The faster crystallizing ability makes the PBT polymer amenable to processing methods like injection molding. On blending PBT with PET, the density drop shifts to an intermediate cooling rate of  $\sim 50$  K/s, useful for faster processing techniques. As shown in Figure 1, the crystallizing ability of the blend is further extended by the presence of plasticizer. For the blend with 5 wt % of [P] and [D] plasticizer, the drop of density is shifted to a higher cooling rate of  $\sim 250$  K/s, and the solidification behavior becomes comparable to that of PBT. Another striking point from the solidification curve (Figure 1) is that the effect on crystallizability is more pronounced for the sample with the [P] plasticizer than the [D] plasticizer. This is because the plasticizers containing long aliphatic chains are more flexible and effective than those containing bulky cyclic phthalate groups.<sup>36–38</sup> In [D] plasticized blends, the amorphous density, observed at the high-cooling-rate plateau, is low compared to those of [P] plasticized blends and is attributed to the added free volume created by the bulky phthalate group.

In this context, it is important to point out that the effect of plasticizer amount on the solidification of the PBT/PET blend is quantitatively observed only for an addition of 5% w/w, while for 1%, in Figure 2, the action is not observed to any measurable extent. The data in this same figure point out the remarkable reproducibility of the density data, which refer to samples of different compositions that have undergone all of the successive steps for preparation (cryomilling, hot melt film,

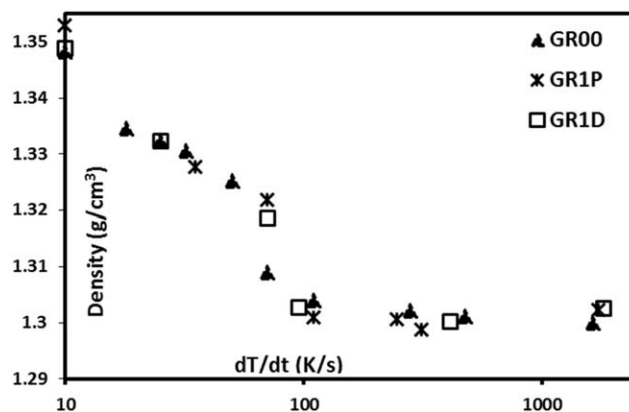


**Figure 2.** Solidification curves of the blends GR00, GR1P, and GR1D. Influence of lower plasticizer content: 1% w/w of both plasticizing agents [D] and [P]; see text.

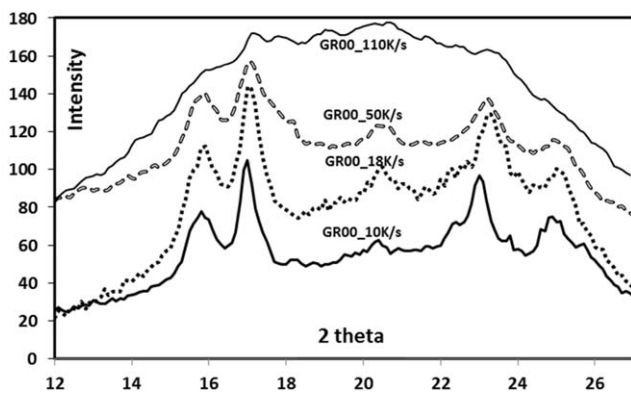


**Figure 3.** WAXD pattern of the unplasticized blend quenched at different cooling rates.

solidification at the reported cooling rates) and characterization as reported in the experimental section.

The WAXD pattern of the blend and the plasticized ones are in accordance with the density data, making the two methods consistent and leading to cross-checking of the results. The density does not provide any information on discriminating between the contributions of different phases, but the WAXD patterns to an extent can reveal the distinctive phases and structural features.<sup>39</sup> The qualitative analysis of WAXD data from Figure 3 and Figure 4 shows that the blend displays a distinct crystalline pattern up to a cooling rate of 50 K/s, whereas the plasticized ones have a crystalline order even at a cooling rate of  $\sim 250$  K/s; above this cooling rate the material tends to be substantially amorphous. A more quantitative analysis of the WAXD patterns was attempted by a deconvolution procedure,<sup>39</sup> showing that the results were in line with the solidification curve, and one can reasonably assume that the drop in density is related to the decrease in the total crystalline content when the cooling rate is increased.<sup>11</sup> Thus, the density drop at 50 K/s in blends and 250 K/s in the plasticized material is associated with the transition from a long-range crystalline order to a less-ordered mesomorphic<sup>40</sup> or amorphous phase. However, separation of the crystalline peaks, which are related to the crystalline phases of PET and PBT, is very difficult, due to the close positions of the most intense peaks<sup>21,23</sup> and to the broadening induced by

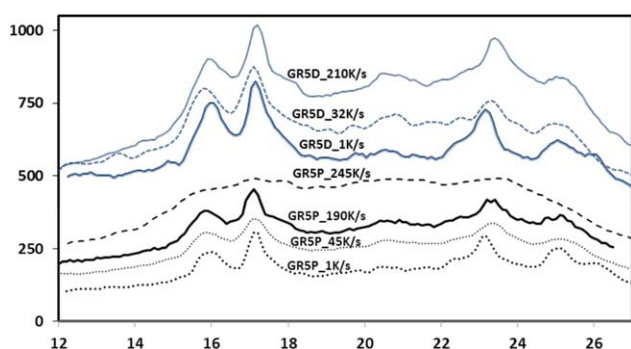


**Figure 4.** WAXD patterns of the plasticized blends quenched at different cooling rates. [Color figure can be viewed in the online issue, which is available at wileyonlinelibrary.com.]

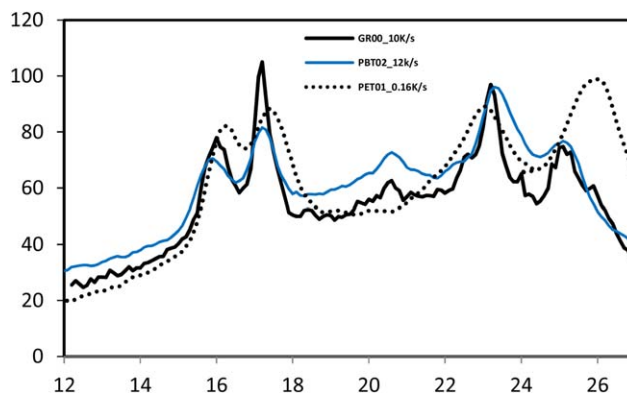


**Figure 5.** Comparison of the WAXD pattern of the blend GR00 and the pure components PBT and PET. [Color figure can be viewed in the online issue, which is available at wileyonlinelibrary.com.]

disorder in the crystalline phases and small crystal dimensions determined by the drastic solidification conditions<sup>39</sup> (Figure 5).

On solidification, the crystalline phase develops from a homogeneous melt. The amorphous miscibility of the blend, mainly speculated from the glass-transition temperature ( $T_g$ ) measurements by DSC or DMTA, confirming earlier observations<sup>5</sup> (Table II and Figure 6) once a single glass transition is observed for all of the blends under investigation. On the other hand, it must be mentioned that the possibility of co-crystallization is excluded in PBT/PET blends, due to incompatible unit cells,<sup>4</sup> and the blend shows all of the characteristic WAXD peaks for PET and PBT (Figure 5); the more distinctly separated they are, the smaller the cooling rate. Upon increasing the cooling rate, however, the PET fingerprints associated with the peaks at  $22.9^\circ$  [(110) reflection] and  $25.9^\circ$  [(101) reflection] tend to disappear, suggesting a decreasing contribution of PET to the onset of its own crystalline phase contribution. The observation is in clear contradiction to the larger density observed in the blend with respect to the simple assumption that volume additivity holds<sup>25</sup>; see Figure 7. The line in bold, identified as the “ideal model,” was indeed calculated on the basis of

$$V_{blend} = \varphi_{PBT} V_{PBT} + \varphi_{PET} V_{PET} \quad (1)$$

where  $\varphi_i$  are the volume fractions and  $V_i (= 1/\rho_i)$  the specific volumes at each cooling rate for each individual constituent, eventually interpolated from empirical fits at cooling rates where that of the blend is calculated.

This observation may be explained only by the incorporation of both PET and PBT moieties in a crystalline phase of increased disorder, in agreement with the broadening of the WAXD peaks.<sup>41</sup>

An accurate DSC analysis of the blend<sup>11</sup> shows two separate peaks for the crystallization of PBT and PET up to relatively low cooling rates, about 60 K/min (1 K/s), comparable to the lowest adopted in this work with the CCT procedure. The DMTA data reported in Figure 6 confirm a single glass transition for the moieties of PBT and PET, determined by the common amorphous mobile phase. Observation of the significant lowering of the  $T_g$  of the plasticized blend with respect to the unplasticized

**Table II.** The glass transition ( $T_g$ ) and crystallization temperature ( $T_c$ ) Data from DSC and DMTA

Sample	$T_g$ (°C) DSC	$T_g$ (°C) DMTA	$T_c$ (°C) 1st Cool	$T_c$ (°C) 2nd Cool
PBT	35	30	187	188
PET	76	74	210	210
GR00	45	45	195	187
GR5P	45	32	193	180
GR5D	45	36	193	183

one is relevant to the results of Figure 6, with a small difference due to the presence of the two plasticizers, as summarized in Table II, where  $T_c$  is the crystallization temperature from DSC. The difficulty of measuring the glass transition on PBT stems from the poor S/N of the stress signal that is due to the significant drop of sample modulus. The initial step in  $\tan \delta$  of the plasticized blends, close to the noisy upswing observed for PBT, suggests their glass transition becomes closer to that of PBT, as the  $T_g$  data of Table II confirm.

#### Effect of Cryogenic Grinding on the Solidification of Blends

The mixing methodology can greatly affect the properties of polymer blends.<sup>42</sup> The influence on the solidification behavior of PBT/PET blends has already been suggested in a previous work. The commercial blend showed consistently larger densities than the lab-scale blend prepared from a Brabender-type internal mixing of pelletized pure polymers.<sup>11</sup> The effect of grinding, before melt mixing, on the solidification curve of the blends is shown in Figure 7, where all density values must be read on the left-hand axis except for PET, which is reported on the right-hand axis. The ideal model, also shown in Figure 7 by the thicker continuous line, is obtained by Equation (1) based on data of the pure components at the same cooling rate.<sup>11</sup>

The intermediate-cooling-rate range is the most interesting one because moving the density drop to larger cooling rates implies an extension of the crystallization range. First of all, a sharper density drop is observed for the unground blend RW00 than for the ground one (GR00). Furthermore, in GR00 the density drop

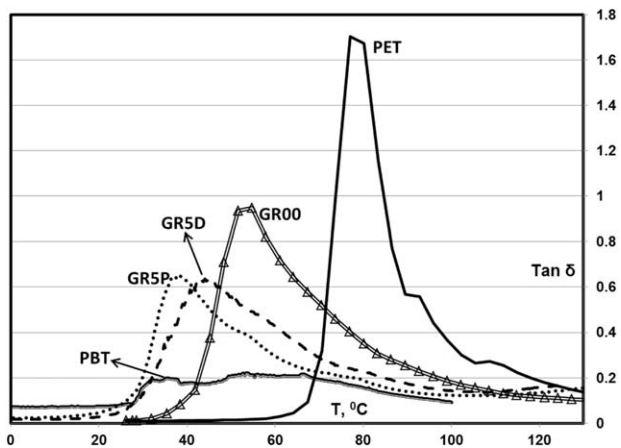


**Figure 6.**  $\tan \delta$  from the DMTA scan for the blends and pure components.

occurs at a cooling rate larger than that of the unground one, showing that crystallization is favored in blends where grinding of the pelletized components anticipates the melt blending, a result of the improved dispersion obtained by the smaller particle size, determining the homogeneity of the feed and providing better contact among the individual components.<sup>43,44</sup>

The featureless trend observed for the unground RW00 becomes much more interesting for the ground GR00, where one can clearly observe two distinct density drops, one around  $\sim 10$  K/s and a second one in the  $\sim 50$  K/s region. PET is a slow-crystallizing material, and it is amorphous above  $\sim 2$  K/s. The density data of the ground blend, GR00, upon comparison with the solidification curve of PET, suggest that the crystallization of PET takes place up to cooling rates of  $\sim 10$  K/s, followed by a drop in density. As discussed in the following, where co-crystallization in an extended cooling-rate range is explained, in this intermediate cooling-rate range between 10 and 50 K/s, being the blend density larger than the value corresponding to the volume mixing rule (eq 1) as shown in Figure 7, must depend on the inclusion of PET moieties in the crystalline phase, which consequently withstands larger disorder, as the broadened WAXD patterns of Figure 3 confirm.

The second drop in density in the ground GR00 blend is observed around  $\sim 50$  K/s because above this cooling rate a density plateau is observed to be related to the disappearance of any long-range crystalline phase, the blend becoming amorphous, as confirmed by the WAXD patterns of Figure 3. Such a clear-cut, separate density drop, which can be due to a significant decrease in the amount of PET and PBT crystallites, could not be seen in the unground blend, RW00, where only one density drop is observed around 40 K/s. In Figure 7 the same effect can also be seen for the blends with plasticizers, GR5P, where the grinding is accompanied by a double density drop, similar to the unground GR00 blend, which is further shifted to a higher cooling rate than GR00, with respect to the unique drop-off of density observed in the unground blend RW5P.

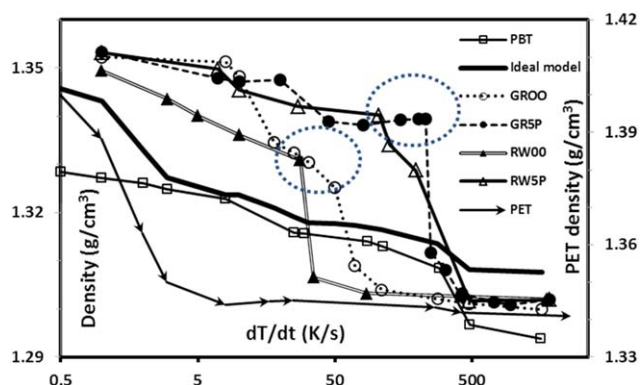


**Figure 7.** Influence of cryogenic grinding on the solidification curve. Pure components PET, PBT, and “ideal” model obtained by eq. 1, on a 60/40 w/w basis, are compared to the ground blends GR00 and GR5P and the unground ones RW00 and RW5P, where 5P implies 5% w/w of PEGDME plasticizer. All density values must be read on the left-hand axis except for PET, which is reported on the right-hand axis. [Color figure can be viewed in the online issue, which is available at [wileyonlinelibrary.com](http://wileyonlinelibrary.com).]

Grinding not only extends the range where crystallization occurs, albeit slightly, but it also improves the description of the solidification curve implying more accurate results.

The most significant extension of the crystallization range is, however, observed in Figure 7 after the addition of the plasticizers. In the case of the plasticized and ground blend, GR5P, the first drop-off of density, associated with the disappearance of crystallites of PET separated by PBT, shifts to a larger cooling rate: from 10 K/s for GR00 to about 40 K/s for GR5P. The synergy between plasticizer action and grinding is shown by the extension of the crystallization range before the onset of the amorphous phase, which moves from about 50 K/s for GR00 to above 400 K/s for GR5P. In this range, we attribute the onset of the crystalline phase to the inclusion of both PET and PBT moieties in the crystalline phase, as suggested by the broadened patterns of Figure 4 and explained by the possible occurrence of large amounts of structural disorder and in the absence of true three-dimensional long-range order.<sup>41</sup> The pulverization process thus increases the specific surface area of the components before mixing, improving the degree of dispersion and the plasticizing action.<sup>45</sup>

## DISCUSSION AND CONCLUSION

The methodology adopted to study the solidification behavior of blends of commercial and technological relevance gives access to information not otherwise available by other solidification methods. It describes the solidification behavior in terms of macroscopic density versus the relevant cooling rate adopted, the so-called “solidification curve.”<sup>19</sup> Ancillary information is collected point-wise from WAXD patterns, which, providing a qualitative description of the crystalline phases formed, confirm and complete the description of the solidification behavior in a broad range of cooling conditions, comparable to those experienced in polymer processing.

Most important from a technological viewpoint is the notion that plasticizers extend the operating window of materials not otherwise available to processing methods where drastic solidification conditions are encountered, such as injection molding. Figure 1, however, shows that there is a difference in their action because an oligomeric plasticizer is more effective than a bulky one, leading us to speculate and invoke mechanisms yet to be proven in this particular case.

In particular, it is known that low molar masses improve the rheological behavior of polymer blends that are eventually added or present due to the broad mass distribution. The mechanism responsible for the extended solidification behavior could thus be associated with the constraint release induced by low-molar-mass species where the release rate of undiluted entanglements is accelerated by the diffusing diluent.<sup>46,47</sup> In this context, we believe the crystallization of polymer blends has itself important implications for the mechanism of solidification, explaining the role of plasticizers and justifying some observations not in line with the secondary nucleation mechanism of polymer crystallization.

Indeed, the mentioned miscibility of PET and PBT in the melt,<sup>5</sup> confirmed in Figure 6 by the unique glass transition shown for all of the blends studied, joined to the reported incompatibility of the unit cells of PET and PBT, implies that a preliminary step of demixing in the liquid before attachment to the

“different” growing crystalline phases must take place. Certainly this step is rate determining, so if it takes place it does so to the extent compatible with the cooling rate adopted. For example, this step implies a separation of the two moieties at a scale compatible with the crystalline stem length of each moiety followed by attachment to the closer-growing compatible crystalline phase. This perspective is clearly incompatible with the notion of entangled melts because their accumulation in the non-crystalline domains upon solidification is itself a deterrent to the onset of a crystalline phase. This observation is clearly dependent on local mobility and therefore on time: if mobility is enhanced by one of the mechanisms invoked previously, massive segregation can take place, determining a local fractionation due to selective separation of the two moieties driven by the onset of stable and optimized separate crystalline phases, whose size is thermodynamically determined and which the crystallization temperature.<sup>48</sup> In this case, one observes well-separated crystalline peaks clearly attributed to the two incompatible crystalline phases. However, such a situation should arise only for low cooling rates, below the first density drop where PET crystallization is responsible for the larger density. Above this threshold, located at around 10 to 50 K/s, depending on plasticizer content, it is plausible that another scenario takes place, as shown by the broadened WAXD patterns well explained by Corradini.<sup>41</sup> There the concepts of crystallinity and crystals in synthetic macromolecules are interpreted as a concomitant occurrence of large amounts of structural disorder and in the absence of true three-dimensional, long-range order. This concept explains the unusual ability of polymers to crystallize even in the presence of a high degree of structural disorder. In such a situation, dichotomizing just for the sake of simplification, when cooling rates are large and time is short, segregation does not occur, and more disordered crystals form, as pointed out by the broader WAXD peaks of Figures 3–5.

Segregation on polymer crystallization is known to occur in many circumstances,<sup>49,50</sup> all related to either long solidification times or relatively small molar masses, which are eventually expelled from the growing crystal phase as the molecular nucleation mechanism prescribes.<sup>51</sup> The mechanism is so effective that it can be used for fractionation,<sup>52</sup> and it is known to significantly affect mechanical properties<sup>53,54</sup> by reducing the density of entanglements.

In a previous work, some of the data presented here and from the literature were compared with the ratio of two molar masses as an index of local mobility during crystallization: the molar mass between adjacent entanglements and that of a crystalline stem.<sup>25</sup> The ratio being large in PE, about 8<sup>25</sup>, it allows, for low molar masses, segregation to be effective even for high cooling rates: the drop-off of density is not observed even above 1000 K/s.<sup>55</sup> In the case of more rigid chain polymers like PET, where the ratio barely reaches a value of 2, its sensitivity to the addition of effective diluents on the solidification under processing conditions is dramatic, as the results presented in this work show: PET, a low-cost polymer, barely crystallizable under mild solidification conditions, becomes suitable to processing even by injection molding by blending with PBT and through the addition of low-molecular-weight species purposely added as the oligomeric PEDGME plasticizer studied in this work.

## ACKNOWLEDGMENTS

We gratefully acknowledge the Italian Ministry of Education for financial support under the PRIN grant scheme and the University of Palermo for the Ph.D. fellowship of A.M.P.

## REFERENCES

1. Liu, L. Z.; Chu, B.; Penning, J. P.; Manley, R. *St. Macromolecules* **1997**, *30*, 4398.
2. Liu, J.; Jungnickel, B. J. *J. Polym. Sci. Pol. Phys.* **2007**, *45*, 1917.
3. Jungnickel, B. J. In *Polymer Crystallization: Observations, Concepts and Interpretations*; G. Reiter, J. U. Sommer, Eds.; Springer: Heidelberg, Germany, **2003**, Vol. 606, p 208.
4. Escala, A.; Stein, R. S. *Adv. Chem. Ser.* **1979**, *176*, 455.
5. Avramova, N. *Polymer* **1995**, *36*, 801.
6. Yu, Y.; Choi, K. *J. Polym. Eng. Sci.* **1997**, *37*, 91.
7. Gargand, S. N.; Misra, A. *Makromol. Chem Rapid. Commun.* **1981**, *2*, 241.
8. Mishra, S. P.; Deopura, B. L. *Makromol. Chemie* **1985**, *186*, 641.
9. Font, J.; Muntasell, J.; Cesari, E. *Mater. Res. Bull.* **1999**, *34*, 157.
10. Aravinthan, G.; Kale, D. D. *J. Appl. Polym. Sci.* **2005**, *98*, 75.
11. Stocco, A.; La Carrubba, V.; Piccarolo, S.; Brucato, V. *J. Polym. Sci. Pol. Phys.* **2009**, *47*, 799.
12. Maruhashi, Y.; Iida, S. *Polym. Eng. Sci.* **2001**, *41*, 1987.
13. Szostak, M. *Mol. Cryst. Liquid Cryst.* **2004**, *416*, 209.
14. Sperling, L. H. *Polymeric Multicomponent Materials: An Introduction*; Wiley-Interscience: New York, **1997**.
15. Guo, M.; Brittain, W. J. *Macromolecules* **1998**, *31*, 7166.
16. Alexandrova, L.; Cabrera, A.; Hernandez, M. A.; Cruz, M. J.; Abadie, M. J. M.; Manero, O.; Likhatchev, D. *Polymer* **2002**, *43*, 5397.
17. Backson, S. C. E.; Kenwright, A. M.; Richards, R. W. *Polymer* **1995**, *36*, 1991.
18. Matsuda, H.; Asakura, T. *Macromolecules* **2002**, *35*, 4664.
19. Brucato, V.; Piccarolo, S.; La Carruba, V. *Chem. Eng. Sci.* **2002**, *57*, 4129.
20. Poulouse, A. M.; Piccarolo, S.; Carbone, D. AIP Conference Proceedings. Times of Polymers and Composites; American Institute of Physics; Melville, New York, **2010**; p 209. <http://scitation.aip.org/content/aip/proceeding/aipcp/10.1063/1.3455582>
21. Asano, T.; Baltá Calleja, F. J.; Flores, A.; Tanigaki, M.; Mina, M. F.; Sawatari, C.; Itagaki, H.; Takahashi, H.; Hatta, I. *Polymer* **1999**, *40*, 6475.
22. Raabe, D.; Chen, N.; Chen, L. *Polymer* **2004**, *45*, 8265.
23. Liuand, J.; Geil, P. H. *J. Macromol. Sci. Phys.* **1997**, *36*, 263.
24. Stein, R. S.; Khambatta, F. B.; Warner, F. P.; Russell, T.; Escala, A.; Balizer, E. *Polym. Sci. Polym. Sym.* **1978**, *63*, 313.
25. Piccarolo, S.; Poulouse, A. M.; Luzio, A. *J. Appl. Polym. Sci.* **2012**, *125*, 4233.
26. Gowd, E. B.; Ramesh, C. *Polym. Int.* **2006**, *55*, 340.
27. Piorkowska, E.; Kulinski, Z.; Galeski, A.; Masirek, R. *Polymer* **2006**, *47*, 7178.
28. Yang, S. L.; Wu, Z. H.; Meng, B.; Yang, W. *J. Polym. Sci. Pol. Phys.* **2009**, *47*, 1136.
29. Michael, S.; Uwe, K. *Colloid Polym. Sci.* **2004**, *282*, 381.
30. Zhu, Y. G.; Li, Z. Q.; Zhang, D.; Tanimoto, T. *J. Appl. Polym. Sci.* **2006**, *99*, 2868.
31. Brucato, V.; Piccarolo, S.; Titomanlio, G. Analysis of Non-Isothermal Crystallization Kinetics of PET. European XI PPS Meeting Proceeding, Hanser (Berlin, Germany) **1995**; p 530.
32. Piccarolo, S.; Brucato, V.; Kiflie, Z. *Polym. Eng. Sci.* **2000**, *40*, 1263.
33. Kiflie, Z.; Piccarolo, S.; Brucato, V.; Baltá-Calleja, F. *J. Polymer* **2002**, *43*, 4487.
34. Piccarolo, S.; Vassileva, E.; Kiflie, Z. In *Polymer Crystallization: Observations, Concepts and Interpretations*; G. Reiter, J. U. Sommer, Eds.; Springer: Heidelberg, Germany, **2003**; p 325.
35. Aharoni, S. M. *Macromolecules* **1983**, *16*, 1722.
36. Baltieri, R. C.; Innocentini Mei, L. H.; Bartoli, J. *Macromol. Symp.* **2003**, *197*, 33.
37. Woo, L.; Cheung, Y. W. *Thermochim. Acta* **1990**, *166*, 77.
38. Wypych, G. *Handbook of Plasticizers*, 2nd ed.; ChemTec: Toronto, Canada, **2012**.
39. Martorana, A.; Piccarolo, S.; Scichilone, F. *Macromol. Chem. Phys.* **1997**, *198*, 597.
40. Zia, Q.; Androsch, R.; Radusch, H. J.; Piccarolo, S. *Polymer* **2006**, *47*, 8163.
41. Corradini, P.; Auriemma, F.; De Rosa, C. *Acc. Chem. Res.* **2006**, *39*, 314.
42. Utracki, L. A. *Polymer Alloys and Blends: Thermodynamics and Rheology*; Hanser Gardner: Cincinnati, OH, **1990**.
43. Schexnaydre, R. J.; Mitchell, B. S. *J. Polym. Sci. Pol. Phys.* **2008**, *46*, 1348.
44. Mano, J. F.; Denchev, Z.; Nogales, A.; Bruix, M.; Ezquerro, T. A. *Macromol. Mater. Eng.* **2003**, *288*, 778.
45. Bilgili, E.; Arastoopour, H.; Bernstein, B. *Powder Technol.* **2001**, *115*, 265.
46. von Meerwall, E. D.; Dirama, N.; Mattice, W. L. *Macromolecules* **2007**, *40*, 3970.
47. Wang, Z.; Larson, R. G. *Macromolecules* **2008**, *41*, 4945.
48. Strobl, G. *Prog. Polym. Sci.* **2006**, *31*, 398.
49. Prime, R. B.; Wunderlich, B. *J. Polymer Sci. 2 Polymer Phys.* **1969**, *7*, 2061.
50. Hu, W. *Macromolecules* **2005**, *38*, 8712.
51. Wunderlich, B. *Faraday Discuss.* **1979**, *68*, 239.
52. Anantawaraskul, S.; Soares, J. B. P.; Wood-Adams, P. M.; Monrabal, B. *Polymer* **2003**, *44*, 2393.
53. Plummer, C. J. G. *Adv. Polym. Sci.* **2004**, *169*, 75.
54. Gedde, U. W.; Jansson, J. F. *Polymer* **1985**, *26*, 1469.
55. Sapoundjieva, D.; Piccarolo, S.; Martorana, A. *Macromol. Chem. Phys.* **2000**, *201*, 2747.